JPC-B103-4399-Hirakawa-Primary-lumino

DATASET · JULY 2013

READS
34

4 AUTHORS, INCLUDING:

Sittidej Teekateerawej
Nagaoka University of Technology
19 PUBLICATIONS **100** CITATIONS

SEE PROFILE

Primary Passages for Various TiO_2 Photocatalysts Studied by Means of Luminol Chemiluminescent Probe

Tsutomu Hirakawa, Yasuhiro Nakaoka, Junichi Nishino, and Yoshio Nosaka*,†

Department of Chemistry, Nagaoka University of Technology, Kamitomioka, Nagaoka 940-2188, Japan

Received: October 21, 1998; In Final Form: March 9, 1999

Photocatalytic properties of TiO_2 aqueous suspension were analyzed by means of the chemiluminescent probe method, which enables us to monitor superoxide ions ($^{\bullet}O_2^-$) and hydrogen peroxide (H_2O_2) in the reaction system. The amount of produced $^{\bullet}O_2^-$ is independent of the surface properties of TiO_2, while H_2O_2 is formed significantly for smaller particles with large amount of surface hydroxyl groups. The amount of produced $^{\bullet}OH$ radicals was estimated from the effect of Cl^- ions on the $^{\bullet}O_2^-$ formation and found to be large for the TiO_2 having a large amount of surface hydroxyl groups. This difference is explained to originate from the different structure of hole intermediates, based on the ESR measurements for these powders at 77 K.

Introduction

Photocatalytic reaction by using semiconductor powder has been paid much interest because of its practical applications to the clean-up of building materials and the mineralization of waste water.[1] In photocatalysis, light irradiation on semiconductor powder with an energy more than its band-gap energy produces electrons (e^-) and holes (h^+) in conduction band and valence band, and they have abilities to reduce and oxidize the molecules at the surface, respectively. For the reaction under ambient condition, active oxygens such as hydroxyl radicals ($^{\bullet}OH$), superoxide ions ($^{\bullet}O_2^-$), and hydrogen peroxide (H_2O_2) have been noticed as key species to proceed the reaction.[2] These oxygen species are formed in reactions 1−4), where, HO_2^- is

$$e^- + O_2 \rightarrow {}^{\bullet}O_2^- \quad (1)$$

$$h^+ + OH^- \rightarrow {}^{\bullet}OH \quad (2)$$

$$^{\bullet}OH + {}^{\bullet}OH \rightarrow H_2O_2 \quad (3)$$

$$^{\bullet}O_2^- + e^- + H_2O \rightarrow HO_2^- + OH^- \quad (4)$$

an ionized form of hydrogen peroxide H_2O_2 having p$K_a$of 11.7. In our previous report,[3] the authors have described the first application of chemiluminescent (CL) probe to the photocatalytic reactions in aqueous suspension of a sort of semiconductor powder and showed that two CL processes concerning $^{\bullet}O_2^-$ and H_2O_2 could be distinguished. Recently, the CL probe method has also been applied to the photocatalytic reaction at TiO_2 films exposed to air.[4]

In the present study, we will extend the CL probe method to estimating the contribution of luminol oxidation and apply this method successfully to several kinds of TiO_2 powders available commercially as photocatalysts. The results clearly indicate that the initial oxidation passage is affected significantly by the surface properties of TiO_2 powders. It will be also clarified that the difference originates from the formation of different kind of hole intermediates which could be distinguished by means of the photoinduced ESR (electron spin resonance) spectroscopy for the powders at 77 K.[5]

Experimental Section

Materials and Characterization. The TiO_2 powders used were Degussa P25 (Japan Aerosil), Hombikat UV100 (Sachtleben Chemie), ST-01 (Ishihara Techno), F4, and F6 (Showa Titanium). All powders were generous gifts from the corresponding manufacturers.

In order to know the primary particle size and the crystalline composition of these powders, X-ray diffraction (XRD) of the TiO_2 powders was measured with a Rigaku GeigerFlex RAD III. Surface area was measured by the BET method with a Micromesotechs flow sorb (Shimadzu 2300) with N_2 as the adsorbate. Thermogravity (TG) was measured with a TG-DTA meter (Seiko SSC/5200) for the estimation of the amount of surface OH groups. It was calculated as the relative decrement of the weight from 150 to 600 °C.

The secondary particle size of TiO_2 suspended in 0.01 M (M = mol dm^{-3}) NaOH solution was measured as the mean Stokes diameter with a centrifugal size distribution meter (Shimadzu SA-CP3). Surface ζ potential at pH 11.0 was obtained as an average value of 30 particles measured by means of electrophoresis.

For ESR measurements, the TiO_2 powder was placed in an ESR sample tube of 5 mm diameter, and then it was evacuated and sealed. The measurements were carried out at 77 K with a JEOL ES-RE2X ESR spectrometer under photoirradiation with a 500 W mercury lamp (Ushio USH 500D) through a band-pass filter (Toshiba UV-D36C).

Method of Chemiluminescence Probing. The sample for CL measurements was TiO_2 aqueous suspension in 3.5 mL (L = dm^3) solution of 0.01M NaOH. The amount of TiO_2 powder was 15 mg unless otherwise described. The TiO_2 suspension of pH 11.0 was stirred with a magnetic bar in a Pyrex cell (1 cm × 1 cm) placed in a dark box. Aqueous solution (50 μL) of 7 mM luminol was added with a syringe into the solution. We named the procedures as preaddition and post-addition, corresponding to the experiments where luminol is added before and after the irradiation, respectively. Irradiation

† E-mail: nosaka@nagaokaut.ac.jp. Fax: +81-258-47-9315.

10.1021/jp9840984 CCC: $18.00
Published on Web 04/30/1999

at the wavelength of 387 nm was performed with a 150 W xenon lamp (Hamamatsu Photonics Ltd. C2499) through two glass filters (Hoya, U-330 and L39). The irradiation light was confined in the wavelength region so as to be absorbed only in TiO_2. After the irradiation light was switched off with a shutter, CL was monitored with a photon-counting photomultiplier tube (Hamamatsu, R2949), where photons were counted in consecutive 1024 channels of 20 ms gate. Other details of the experimental setup have been described previously.[3]

Several experimental schemes for the irradiation of light and the addition of reagents were performed. The method of irradiation can be classified into two types: single irradiation and multiple irradiation. In the multiple irradiation, the irradiation period was 10 s and the interval between irradiations was about 40 s including the monitoring time of 20 s.

There are two chemiluminescent reactions, (5) and (6), where,

$$^{\bullet}L^{-} + {}^{\bullet}O_2^{-} + H^{+} \rightarrow LO_2H^{-} \quad (5)$$

$$L + HO_2^{-} \rightarrow LO_2H^{-} \quad (6)$$

$^{\bullet}L^{-}$ and L are luminol radical and two-electron oxidized luminol, respectively. The reaction product, LO_2H^{-}, rapidly decomposes into the excited state of 2-aminophthalate which emits light at around 425 nm. The CL intensity measured as the number of photons in 20 ms is proportional to the rate of LO_2H^{-} formation, and then it is proportional to $[^{\bullet}L^{-}][^{\bullet}O_2^{-}]$ for reaction 5 and $[L][H_2O_2]$ for reaction 6. Note that $[HO_2^{-}]/[H_2O_2] = 0.20$ at pH 11.0 because the pK_a of H_2O_2 is 11.7. The time profile of the CL intensity was analyzed by tracing the decay with a computer to be two decay components:[3] fast decay component and slow decay component. The fast one is exponential decay with a decay rate of about 1 s^{-1}, and the slow one is almost second-order decay with a decay rate of 0.1−0.3 s^{-1}, depending on the amount of $^{\bullet}L^{-}$. The time profiles of the fast and slow decay components follow $[^{\bullet}O_2^{-}]$ and [L], respectively, as described below.

The fast decay component is dominant only in the postaddition experiments, where the amounts of H_2O_2 and $^{\bullet}L^{-}$ are very small. The intensity of the fast decay component gives information of $^{\bullet}O_2^{-}$ because the amount of $^{\bullet}L^{-}$ is larger than that of $^{\bullet}O_2^{-}$. Kinetic simulation in the previous report[3] shows that the decay profile of CL in the postaddition experiment is almost equal to that of $^{\bullet}O_2^{-}$. Since the amount of $^{\bullet}O_2^{-}$ decreases mainly by the CL reaction with $^{\bullet}L^{-}$, the total number of photons in the fast decay component is proportional to the amount of $^{\bullet}O_2^{-}$ and it is independent of the amount of $^{\bullet}L^{-}$. In order to know the effect of $^{\bullet}OH$ radicals on the amount of $^{\bullet}O_2^{-}$, a small amount of NaCl was added before the irradiation in some postaddition experiments, because Cl^{-} ions react rapidly with $^{\bullet}OH$ radicals.

The slow decay component of CL is dominant in the preaddition experiments where TiO_2 was irradiated in the presence of luminol. The CL intensity of only this component was increased by the addition of H_2O_2, indicating that the slow decay component is represented by reaction 6. The time profile of the slow decay component follows the amount of L, because $[L] << [HO_2^{-}]$. The decay of L, however, mainly occurs by the reaction with OH^{-} ions rather than by the CL reaction with HO_2^{-}. The lifetime was calculated to be 0.25 ms at pH 11.0 and the amount of L at each time could be calculated as the quasi-stationary state formed by the disproportionation reaction of $^{\bullet}L^{-}$.[3] Thus, the total number of photons of the slow decay component is proportional to the amount of L reacting with HO_2^{-}, which is roughly proportional to the total amount of L produced.

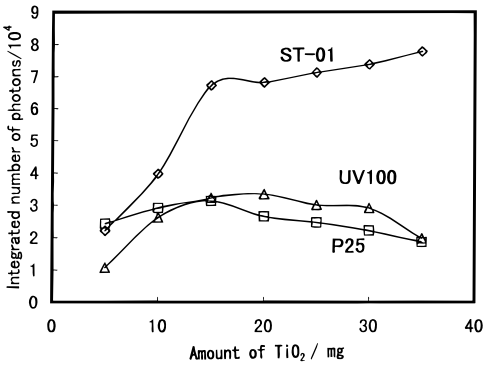

Figure 1. . Number of photons as the chemiluminescence intensity observed during 20 s after the addition of luminol at the end of 60 s irradiation on various kinds of TiO_2 was plotted as a function of the amount of TiO_2 suspended in 3.5 mL of 0.01 M NaOH aqueous solution.

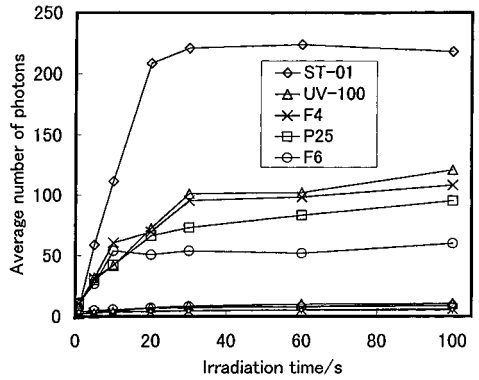

Figure 2. Chemiluminescence intensities of fast decay component (upper curves) and slow decay component (lower curves) observed for several kinds of TiO_2 as a function of irradiation duration.

Results and Discussion

Single Irradiation. Figure 1 shows the CL intensity as a function of the amount of three kinds of TiO_2 powders, where luminol was added after the end of the irradiation (postaddition method). Since the CL intensity does not much depend on the amount of TiO_2, 15 mg was adopted as the amount of TiO_2 in the following experiments.

In Figure 2 are plotted the CL intensities as a function of the period of irradiation time. The CL in the postaddition experiment originates mainly from the fast decay component. Since the CL intensity of the fast decay component is proportional to the amount of $^{\bullet}O_2^{-}$ as described above, the upper curves in Figure 2 illustrate the growth of $^{\bullet}O_2^{-}$ to a certain value in the stationary state under the irradiation. The amount of $^{\bullet}O_2^{-}$ was large for ST-01 TiO_2, while it is small for F6 TiO_2. Among the characteristics of TiO_2 in Table 1, only the secondary particle size shows a substantial difference between ST-01 and UV100. This difference suggests that ST-01 tends to aggregate, although it has the smallest primary size. Then, the formed $^{\bullet}O_2^{-}$ may be stabilized in a cavity among the aggregated crystallites. This explanation seems to be supported by the fact that the lifetime of $^{\bullet}O_2^{-}$ after the irradiation at the surface of TiO_2 film[4] is 50 s in contrast to that of 17 s in aqueous suspension.[3] However, since no significant differences in the lifetime at aqueous suspension was observed between ST-01 and UV100, the lifetime of $^{\bullet}O_2^{-}$ observed after the irradiation may differ from that under the irradiation. The alternative explanation for the

TABLE 1: Properties for the TiO_2 Photocatalysts Used in the Present Study

name of TiO_2	anatase component (%)	primary particle size/nm	BET surface area/-m^2 g^{-1}	secondary particle size/-μm	ζ potential/-mV at pH 11	amount of OH group/wt %
ST-01	100	7	320	3.73	−110	5.2
UV100	100	9	270	0.70	−110	6.0
F-6	80	16	98	0.14	−123	6.1
F-4	90	28	56	1.23	−85	4.9
P25	80	32	49	1.11	−101	1.8
UV100 (500 °C)[a]	100	20	*b*	0.70	*b*	1.3

[a] Heated at 500 °C under H_2 atmosphere for 4 h. [b] Not measured.

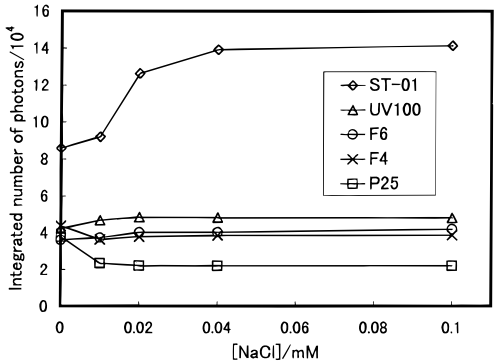

Figure 3. Chemiluminescence intensities observed after single irradiation of 60 s in postaddition method is plotted as a function of the amount of NaCl in the solution.

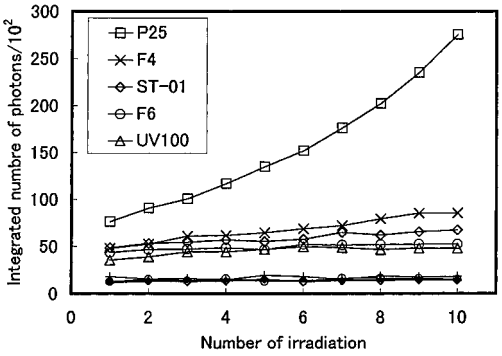

Figure 4. Chemiluminescence intensities of slow decay (upper curves) and fast decay (lower curves) components observed after the repeated irradiations of 10 s plotted as the function of the number of irradiations.

difference in the stationary amount of $^{\bullet}O_2^-$ is the difference in its formation rate. For F6 TiO_2, the crystallite contains chlorine atoms as an impurity, which may become a recombination center for the photogenerated electron−hole pairs and consequently the formation rate becomes small. Since the difference is small among UV-100, F4, and P25 in Figure 2, we may conclude that the production of $^{\bullet}O_2^-$ is hardly affected by the surface properties of TiO_2.

Addition of NaCI in the Single Irradiation. In the presence of various amounts of chloride ions, CL intensity was measured and plotted in Figure 3 as a function of NaCl concentration. For ST-01, UV100, and F6 TiO_2, with the addition of increasing amount of Cl^- ions, the CL intensity increased in the beginning and reached a steady magnitude. On the other hand, for P25 and F4, the chemiluminescence intensity was decreased with the addition of Cl^- ions. This observation shows that the steady-state concentration of $^{\bullet}O_2^-$ increased or decreased with Cl^- ions, depending on some characteristics of TiO_2 powders.

The effect of I^- ions was similar to that of Cl^- ions, despite the large difference in their oxidation potential.[6] This observation implies that the photocatalytic direct oxidation of halide ions is not correlated with the CL intensity. Then the amount of $^{\bullet}O_2^-$ is likely decreased by the reaction with $^{\bullet}OH$ radicals (7), because the reaction rate is of diffusion limit.[7] This reaction (7) competes against the reaction with holes (8).

$$^{\bullet}O_2^- + {}^{\bullet}OH \rightarrow O_2 + OH^- \quad (7)$$

$$^{\bullet}O_2^- + h^+ \rightarrow O_2 \quad (8)$$

$$Cl^- + {}^{\bullet}OH \rightarrow ClOH^- \quad (9)$$

In the presence of Cl^- ions, $^{\bullet}OH$ radicals react competitively with Cl^- ions (9), because the rate constant is large.[8] Thus, the increase of $^{\bullet}O_2^-$ with Cl^- ions in Figure 3 is explained by the decrease of $^{\bullet}OH$ radicals which can react with $^{\bullet}O_2^-$.

On the other hand, the decrease in the CL intensity with Cl^- ions in Figure 3 can be explained by the following two reaction schemes. Chloride ions in the solution are probably adsorbed on the oxidation site or phototinduced holes (10) and then stabilize the oxidation power of the photocatalysts. Then the amount of $^{\bullet}O_2^-$ in the stationary state decreases by the reaction with $^{\bullet}Cl_{ad}$ (11) as well as the reaction with valence-band holes (8). Another possible process of decreasing CL intensity is the decrease in the formation of $^{\bullet}O_2^-$ (1), since the amount of photoinduced electrons, e^-, is probably decreased by the reaction with the adsorbed Cl atoms (12).

$$Cl^- + h^+ \rightarrow {}^{\bullet}Cl_{ad} \quad (10)$$

$$^{\bullet}O_2^- + {}^{\bullet}Cl_{ad} \rightarrow O_2 + Cl^- \quad (11)$$

$$e^- + {}^{\bullet}Cl_{ad} \rightarrow Cl^- \quad (12)$$

The above consideration leads the conclusion that the photocatalysts which form a large amount of $^{\bullet}OH$ radicals relative to the adsorbed Cl atoms can be designated by the increase in the CL intensity of the fast decay component with the addition of Cl^- ions. Then Figure 3 shows that TiO_2 having relatively large amount of OH groups (ST-01, UV100, and F6) forms large amount of $^{\bullet}OH$ radicals. This conclusion is consistent with the observations[9] at the *in situ* ESR measurements for the photocatalytic decomposition of acetic acid.[10] This approach showed that $^{\bullet}OH$ radicals mediate the oxidation of acetic acid at the surface of UV100 TiO_2 while it was directly oxidized at the surface of P25 TiO_2 powder.[9]

Multiple Irradiation. Figure 4 shows the CL intensity observed after each irradiation on TiO_2 where luminol has been added in advance (preaddition experiment). The fast decay component is relatively small and shows no difference among the photocatalysts used in this experiment. This observation is consistent with that in the single irradiation experiment discussed in the previous section. On the other hand, the slow decay component shows significant difference in the intensity of CL, where P25 TiO_2 causes a large increase with the number of irradiations. The intensity of the slow decay component is

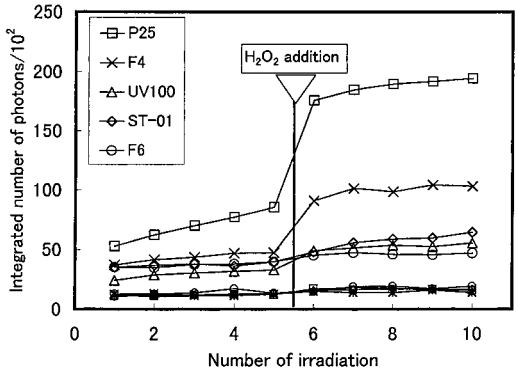

Figure 5. Similar experiment to Figure 4, except that 0.2 mM of H_2O_2 was added after the fifth irradiation in the repeated irradiation scheme.

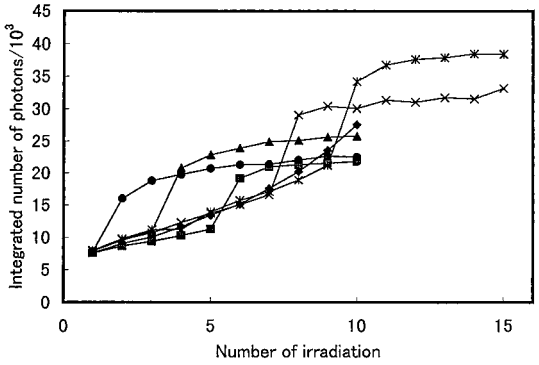

Figure 6. Change in the CL intensity with the number of irradiations for P25 TiO_2 superimposed for the various timings of the addition of H_2O_2; 1 (◆), 3 (▲), 5 (■), 7 (×), and 9(∗).

proportional to $[L][H_2O_2]$ as described above and the time profile of the intensity follows [L]. In the multiple irradiation experiment using the preaddition method, since $^{\bullet}L^-$ radicals have been produced photocatalytically, a large amount of L is formed. On the other hand, the postaddition method in the single irradiation experiment causes a very small amount of L, because $^{\bullet}L^-$ radicals are formed by autoxidation with air.

Addition of H_2O_2 in the Multiple Irradiation. Figure 5 shows that the slow decay component of CL intensity increases with the addition of 0.2 mM of H_2O_2. For ST-01 TiO_2 we reported a similar experiment previously and analyzed for the kinetics.[3] The increment of the CL intensity originates from the increased concentration of H_2O_2. Since the amount of the H_2O_2 added was the same for all the photocatalysts, the difference in the increments observed for each TiO_2 corresponds to the difference in the amount of L. Then, the photocatalyst having larger production of L in Figure 5, such as P25 TiO_2, gives the larger growth with the number of irradiations in Figure 4. Here, the amount of L means the stationary amount, because it decreases on reaction with OH^- and it is supplied from $^{\bullet}L^-$ radicals formed by the photocatalytic reaction in 10 s.

To clarify the constancy of [L], the time of H_2O_2 addition, which had been after 5 irradiations, was changed to 1, 3, 7, and 9 irradiations. The observed CL intensities are plotted in Figure 6 and show the same increment regardless when H_2O_2 was added. Thus, the increment in the CL intensity by the addition of H_2O_2 in Figure 5 can be regarded as the relative amount of oxidized luminol, L, and are plotted in Figure 7 as a function of the amount of OH groups of the corresponding TiO_2. The activity for the luminol oxidation is significantly large at the surface with less OH groups. The amount of H_2O_2 formed by each irradiation could be calculated by comparing the increment in Figure 4 with the step height in Figure 5. That is, the

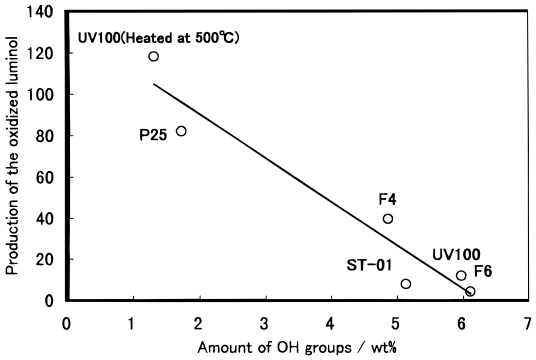

Figure 7. Amount of oxidized luminol (L) produced as the increment of CL intensity with the addition of H_2O_2 observed in Figure 5 plotted as a function of the amount of hydroxyl groups for each TiO_2.

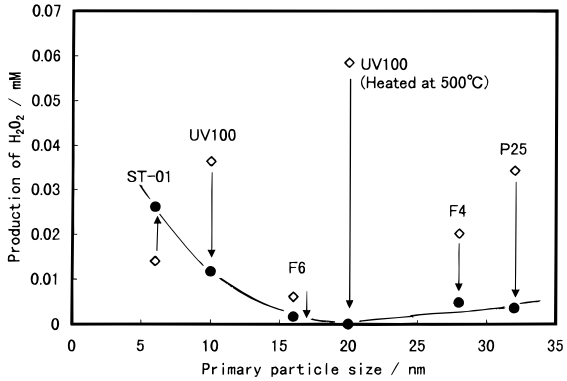

Figure 8. Amount of H_2O_2 produced during each irradiation of 10 s in the presence (◇) and the absence (●) of luminol plotted for six kinds of TiO_2 photocatalysts as the function of the primary particle size.

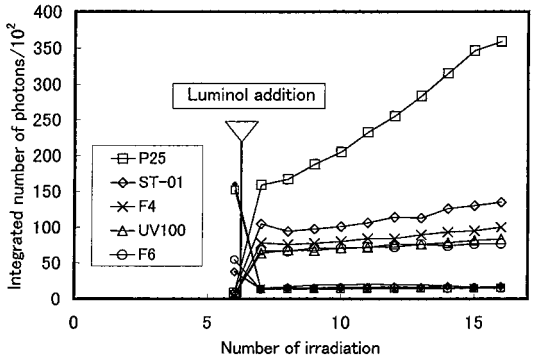

Figure 9. Chemiluminescence intensities of slow decay (upper curves) and fast decay (lower curves) components observed after repeated irradiations of 10 s, where luminol was added immediately after the sixth irradiation.

increment of the slow component in Figure 4 was divided by the relative amount of L shown in Figure 7 and then multiplied by 0.2 mM. Thus the amount of produced H_2O_2 in the presence of luminol was calculated and plotted (diamonds) in Figure 8 as a function of the primary particle size. In order to estimate the intrinsic ability for the H_2O_2 formation of each photocatalyst, the amount of H_2O_2 produced in the absence of luminol was estimated from the following experiment.

Addition of Luminol in the Multiple Irradiation. Figure 9 shows the CL intensity of two decay components observed in the multiple irradiation procedure where luminol was added immediately after the sixth irradiation. When the CL intensity at the seventh irradiation is compared with that of the first irradiation in Figure 4, the amount of H_2O_2 was increased significantly with the six 10 s irradiations in the absence of

luminol. From this difference in the CL intensity, the amount of H_2O_2 produced during one 10 s irradiation was calculated and plotted in Figure 8 with closed circles. The formation of H_2O_2 in the absence of luminol increases at TiO_2 powder of small particle size with large amount of OH groups, such as ST-01 and UV100. On the other hand, the amount of H_2O_2 is very small for TiO_2 of larger particle sizes, such as P25.

The arrows in the figure represent the change in the produced amount of H_2O_2 with the absence of luminol. For only ST-01 TiO_2, the amount of H_2O_2 increased in the absence of luminol. This observation suggests that H_2O_2 is formed from $^{\bullet}OH$ radicals and that the formation of $^{\bullet}OH$ is suppressed by the oxidation of luminol. This explanation agrees with the observation in the experiment of NaCl addition, where large $^{\bullet}OH$ formation is suggested for this particular TiO_2 powder. For other TiO_2 powders, the H_2O_2 formation decreased in the absence of luminol. This observation suggests that the oxidation of luminol is associated with the reduction of O_2 (1), followed by the further reduction (4) or disproportionation to give H_2O_2.

On the basis of the observed amount of H_2O_2, we can estimate the photonic efficiency from the amount of incident light. Two photons absorbed in TiO_2 can produce two H_2O_2 molecules, because H_2O_2 can be produced by the consecutive reduction of oxygen, (1) and (4), as well as the oxidation of OH^- ions (2) followed by the dimerization (3). Then one can calculate that, when the light of 13 mW is absorbed in a suspension of 3.5 mL, 0.12 mM of H_2O_2 can be produced in 10 s as the maximal value. The observed amount of H_2O_2 in Figure 8 suggests that substantial amount of H_2O_2 was formed in the presence of luminol.

Structure of Holes and the Selectivity. In our previous work,[5] we observed the change in the chemical structure of photoproduced holes, where anatase TiO_2 powder (UVIOO) was heat-treated. We showed that this change is caused by desorption of surface hydroxyl groups and consequential change in the surface chemical bonds, because the crystal structure has been preserved by the heating. In the unheated samples possessing a large quantity of surface hydroxyl groups, photogenerated holes produce a paramagnetic species having a set of g values of 2.004, 2.014, and 2.018, which is assigned to the bridge oxygen radical located under the surface Ti atoms, i.e., $Ti^{4+}O^{\bullet-}Ti^{4+}OH^-$.[11] On the other hand, when the hydroxyl groups have been desorbed by heat treatment, the photogenerated holes produce another paramagnetic species having a set of g values of 2.004, 2.018, and 2.030. This radical has been assigned to the terminal oxygen radical located at the surface, $Ti^{4+}O^{2-}Ti^{4+}O^{\bullet-}$,[12] and shows a different reactivity from that of the $Ti^{4+}O^{\bullet-}Ti^{4+}OH^-$ radical,[5] though both radicals can participate in the photocatalytic reaction with the surrounding molecules.

Figure 10 shows the photoinduced ESR spectra for five kinds of TiO_2 powders under vacuum. The shape of the spectra between $g = 2.004$ and $g = 2.030$ changes consecutively from UV100 to P25. When this change is considered with the amount of surface hydroxyl groups in Table 1, the previously concluded relationship is confirmed, where the structure of surface trapped holes changes from $Ti^{4+}O^{\bullet-}Ti^{4+}OH^-$ to $Ti^{4+}O^{2-}Ti^{4+}O^{\bullet-}$ with the decreasing amount of surface hydroxyl groups. Thus, for

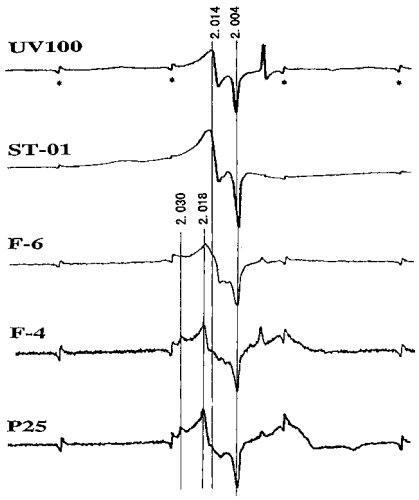

Figure 10. ESR spectra obtained for five kinds of TiO_2 powder under irradiation at 77 K in vacuum. Stars represent the signals of the Mn^{2+} marker.

UV100 and ST-01, the photoinduced holes produce $Ti^{4+}O^{\bullet-}$-$Ti^{4+}OH^-$ radicals, and on the other hand, P25 forms $Ti^{4+}O^{2-}$-$Ti^{4+}O^{\bullet-}$ *d* radicals. Since *OH radicals were formed preferentially on the surface with hydroxyl groups, the trapped holes having the structure of $Ti^{4+}O^{\bullet-}Ti^{4+}OH^-$ may be a precursor of the $^{\bullet}OH$ radical formation.

Acknowledgment. The present work is partly supported by the Grant-in-Aid for Scientific Research (No. 09237105) on Priority-Area-Research of "Electrochemistry of Ordered Interfaces" from the Japanese Ministry of Science, Education and Culture. The authors express their appreciation to Professor K. Uematsu for the use of the electrophoresis apparatus.

References and Notes

(1) Hoffmann, M. R.; Martin, S. T.; Choi, W.; Bahnemann, D. W. *Chem. Rev.* **1995**, *95*, 69−96.

(2) (a) Serpone, N.; Pelizzetti, E.; Hidaka, H. *Photocatalytic Purification and Treatment of Water and Air*; Ollis, D. F., Al-Ekabi, H., Eds.; Elsevier: London, 1993; pp 225−250. (b) Bahnemann, D.; Cunningham, J.; Fox, M. A.; Pelizzetti, E.; Pichat, P.; Serpone, M. In *Auatic Surface Photochemistry*; Helz, G., Zepp, R., Crosby, D., Eds.: CRC: Boca Raton, FL, 1993; pp 261−316. (c) Gerischer, H.; Heller, A. *J. Electrochem. Soc.* **1992**, *139*, 113−118. (d) Gerischer, H. *Electrochim. Acta* **1993**, *38*, 3−9.

(3) Nosaka, Y.; Yamashita, Y.; Fukuyama, H. *J. Phys. Chem. B* **1997**, *101*, 5822−5827.

(4) Ishibashi, K.; Nosaka, Y.; Hashimoto, K.; Fujishima, A. *J. Phys. Chem. B* **1998**, *102*, 2117−2120.

(5) Nakaoka, Y.; Nosaka, Y. *J. Photochem. Photobiol., A*: *Chem.* **1997**, *110*, 299−307.

(6) Nosaka, Y.; Fukuyama, H. *Chem. Lett.* **1997**, 383−384.

(7) Sehested, K.; Rasmussen, O. L.; Fricke, H. *J. Phys. Chem.* **1968**, *72*, 626.

(8) Jayson, G. G.; Parsons, B. J.; Swallow, A. J. *J. Chem. Soc., Faraday Trans. 1* **1973**, *69*, 1597.

(9) Nosaka, Y.; Kishimoto, M.; Nishino, J. *J. Phys. Chem. B* **1998**, *102*, 10279−10283.

(10) Nosaka, Y.; Koenuma, K.; Ushida, K.; Kira, A. *Langmuir* **1996**, *12*, 736−738.

(11) Howe, R. F.; Grätzel, M. *J. Phys. Chem.* **1987**, *91*, 3906.

(12) Micic, O. I.; Zhang, Y.; Cromack, K. R.; Trifunac, A. D.; Thurnauer, M. C. *J. Phys. Chem.* **1993**, *97*, 7277.